

## Second order invariants and holography

Luca Bonanno<sup>¶b</sup>, Gerardo Iannone<sup>b</sup> and Orlando Luongo<sup>‡†§</sup>

<sup>‡</sup>*Dip. di Fisica, Università di Roma "La Sapienza", I-00185 Roma, Italy,*

<sup>b</sup>*Institut für Theoretische Physik, J. W. Goethe - Univ. Max-von-Laue-Straße, 1 60438 Frankfurt am Main, Germany,*

<sup>¶</sup>*Dip. di Fisica, Università di Ferrara and INFN, via Saragat 1, 44100 Ferrara, Italy,*

<sup>†</sup>*Dip. di Scienze Fisiche, Università di Napoli "Federico II", Via Cinthia, Napoli, Italy,*

<sup>§</sup>*Instituto de Ciencias Nucleares, Universidad Nacional Autónoma de México, and*

<sup>b</sup>*Dip. di Fisica, Università di Salerno and INFN, I-84081, Salerno, Italy.*

Motivated by recent works on the role of the Holographic principle in cosmology, we relate a class of second order Ricci invariants to the IR cutoff characterizing the holographic Dark Energy density. The choice of second order invariants provides an invariant way to account the problem of causality for the correct cosmological cutoff, since the presence of event horizons is not an *a priori* assumption. We find that these models work fairly well, by fitting the observational data, through a combined cosmological test with the use of SNeIa, BAO and CMB. This class of models is also able to overcome the fine-tuning and coincidence problems. Finally, to make a comparison with other recent models, we adopt the statistical tests AIC and BIC.

PACS numbers: 98.80.-k, 98.80.Jk, 98.80.Es

### I. INTRODUCTION

Ever since the discovery of the Dark Energy (DE) [1–3], the fundamental problem of understanding the nature of the positive acceleration of the universe appears lacking of some ingredients in the framework of General Relativity (GR). In addition, observations strongly suggest that matter in the universe is dominated by a non-baryonic (cold) dark matter (DM) which seems to evolve separately from the unknown force driving the acceleration [4, 5]. Despite neither DE nor DM have been directly detected, they represent the most relevant amount of energy and matter in the universe, being almost the 70 and 25 percent of the total content, respectively. A theory propounded to explain their effects and to describe their natures is strictly necessary in cosmology, although, up to now, it has not been still definitively formulated [6]. Probably, the most common paradigm trying to include both DE and DM, is the so-called  $\Lambda$ CDM model [7]. In this model, a cosmological constant term,  $\Lambda$ , is included within the Einstein equations and the total matter density is assumed to be the sum of baryonic and DM densities, i.e.  $\rho = \rho_b + \rho_{DM}$ . This model fits excellently and with high-precision all observational data, meanwhile it provides a remarkably small number of cosmological parameters [8]. The effects of  $\Lambda$  are *hidden* in the definitions of the pressure,  $p$ , and of matter density,  $\rho$ , i.e.  $p \rightarrow p + \frac{\Lambda c^2}{8\pi G}$ ,  $\rho \rightarrow \rho - \frac{\Lambda c^2}{8\pi G}$ ; thus, by assuming hereafter a (flat) Friedman-Robertson-Walker (FRW) metrics, i.e.  $ds^2 = c^2 dt^2 - a(t)^2 [dr^2/(1 - kr^2) + \sin^2 \theta d\phi^2 + d\theta^2]$ , we can easily write down the correspondent Friedmann equations:

$$H^2 \equiv \left(\frac{\dot{a}}{a}\right)^2 = \frac{8\pi G}{3}\rho - \frac{kc^2}{R_0^2 a^2}, \quad (1)$$

$$\frac{\ddot{a}}{a} = -\frac{4\pi G}{3}(3p/c^2 + \rho),$$

where  $G$  is the gravitational constant, and  $R_0$  the radius of the universe. If  $p$  and  $\rho$  are known (or equivalently  $H$  is known), the above coupled equations describe the dynamics of the universe.

In spite of its simplicity and its triumph in fitting data, the  $\Lambda$ CDM model suffers from several shortcomings [9], as e.g. the problem of fine tuning and the problem of coincidence. The problem of fine tuning is connected to the large difference between the value of vacuum energy in quantum field theory and the observed value of the cosmological constant [10]. The problem of coincidence is related to the incredibly small differences between the densities of DE and DM, which are supposed to evolve differently as the universe expands. Moreover, one can notice that at large enough energies (typically of the order of the Planck scale,  $M_{pl} \equiv \sqrt{\hbar c/G} \sim 1.22 \times 10^{19} \text{ GeV}/c^2$ ), the  $\Lambda$ CDM model is supposed to be not reliable anymore; in other words, it only provides a limited description [11] of the early stages of the universe. As a consequence, the crucial role played by inflation still remains an effective approach without any basis in a fundamental theory. Nevertheless, a Quantum Gravity (QG) theory seems to be necessary to explain these stages [7], having as a limit the  $\Lambda$ CDM model; that is clear if one believes that GR is a particular case of a more fundamental theory. This is the underlying philosophy of what are usually referred to as modified theories of gravity, concerning the modified Einstein-Hilbert (EH) action [12, 13]. Besides fundamental physics motivations, cosmologists acquired a huge interest in all of these theories, thanks to the possibility to reach a unified scheme. Among the various alternatives, crucial advances have been carried out in the studies of Black Hole theory and String theory [14].

A very intriguing concept, within the framework of GR, is the so-called *holographic principle* (HP), which provides some clues for solving the modern theoretical and observational problems without directly modifying the EH action. As it has been pointed out in QG, the

entropy of a system does not scale with the volume of that system, but with the area of its surface [15]. Starting from the above consideration, the HP postulates that the maximum entropy inside a region is not extensive, but grows as the area of the surface. Therefore, the total number of independent degrees of freedom should scale with the surface area (in Planck units) as well. In particular, the principle invokes that  $L^3 \rho_{vac} \leq LM_{Pl}^2$ , where  $M_{Pl}$  is the Planck mass and  $\rho_{vac}$  is the vacuum energy density of a system of size  $L$ . Actually, the HP represents a new basic principle for both QG and GR, being supported by an effective quantum field theory. In order to include this principle in a real cosmological scenario, one needs to choose the correct cosmological length scale  $L$ , which is not *a priori* known.

Since the cosmological system is the universe, the DE should be associated with the scale density, namely  $\rho_{DE} \equiv \rho_X \propto L$ . Writing the fraction of DE density in the form  $\Omega_X \equiv \frac{\rho_X}{3M_{Pl}^2 H^2}$ , we can imagine different holographic approaches by choosing different IR cutoffs. For instance, for the case of the  $\Lambda$ CDM, if the Hubble parameter  $H$  is taken to be the characteristic scale of the universe, then it is natural to postulate  $\Lambda^{-1/2} \propto H$ ; unfortunately this scenario fails in reproducing the positive acceleration of universe. Nevertheless, from the HP principle, it would be possible to solve both the problems of fine tuning and coincidence just by introducing the correct length scale. In order to fix such a scale, many approaches have been investigated in literature. In the so-called *Holographic Dark Energy model* (HDE) [16, 17] the future event horizon of the universe characterizes the length  $L$ , i.e.

$$L \equiv a \int_a^\infty \frac{da'}{Ha'^2}. \quad (2)$$

An alternative is the so-called agegraphic model (ADE) [18–20], where the IR cutoff is the conformal age of the universe,

$$L \equiv \eta = \int \frac{da'}{a'^2 H}. \quad (3)$$

Unfortunately, the choice of a length scale is neither so easy nor arbitrary, since it leaves unclear some conceptual problems. As pointed out by Cai [21], a drawback, concerning causality, appears in the above scenarios: how is it possible that a local quantity, as e.g. the DE, could be explained by global concepts, derived from the physics of space-time? Is there a mechanism allowing a local quantity to be determined by a global one [22]? A crucial issue is that the above cosmological lengths are originated from an expanding universe, which is an *a priori* assumption and not the result of a certain model, as it should be. In order to solve this problem and inspired by the HP, we suggest to choose as length scales only those quantities which are invariant under geometrical transformations, avoiding the causality issue. This allows to solve both the coincidence and fine-tuning problems, as well. The

invariants of curvature, derived from the Ricci scalar  $R$ , the Weyl tensor  $C_{\mu\nu\xi\delta}$  and the Riemann tensor  $R_{\mu\nu\xi\delta}$ , are based on such theoretical implicit assumptions and represent geometrical invariants. Gao [23] suggested, for the first time, that the DE density could be proportional to the first order invariant  $R$ :<sup>1</sup>

$$\rho_X \propto R. \quad (4)$$

In this work we extend the analysis by Gao to the case of *second order* (independent) invariants. Notice that a second order invariant is proportional to the inverse fourth power of an IR cutoff, then indicating with  $I_i$  the  $i$ -th independent second order invariant, our assumption should be formulated as follows

$$\rho_X \propto \sqrt{|I_i|}. \quad (5)$$

The purpose of the present article is to study the models originating from these invariants and their implications on the FRW spacetime. As shown below, these models fairly overcome the problem of the length scale, providing a good solution for the DE problem [7] and indicating a good agreement with the theoretical predictions.

The paper is organized as follows: in Section II we develop the theory of the independent second order invariants for a flat FRW universe and we analyze the outcomes of the assumption (5) in cosmology. In Section III we fit our models with the cosmological data from Supernovae Ia (SNeIa), Baryonic Acoustic Oscillation (BAO) and Cosmological Microwave Background (CMB). In Section IV, we provide a comparison with other relevant cosmological models and we make use of model independent statistical tests, i.e. the AIC and BIC. Finally in Section V we present the conclusions.

## II. SECOND ORDER HOLOGRAPHIC INVARIANTS

The basic purpose of this work is to invoke the HP and to relate the second order curvature (independent) invariants to the DE density (as already discussed, the case of the first order curvature invariant has been extensively treated by Gao [23–25]).

This can be easily performed by writing down the explicit form of the second order geometrical invariants for a FRW metric and by using eq. (5). As pointed out in Ref.[27], among the 14 curvature scalar invariants [26], the most interesting ones are the Kretschmann, the Chern-Pontryagin and Euler invariants. We can write, for every spacetime [28–32], their expressions as follows

$$\begin{aligned} K_1 &= R_{\alpha\beta\gamma\delta} R^{\alpha\beta\gamma\delta}, \\ K_2 &= [*R]_{\alpha\beta\gamma\delta} R^{\alpha\beta\gamma\delta}, \\ K_3 &= [*R^*]_{\alpha\beta\gamma\delta} R^{\alpha\beta\gamma\delta}, \end{aligned} \quad (6)$$

<sup>1</sup> Usually the model is referred to as the Ricci Dark Energy (RDE) model.

where the stars indicate the correspondent dual counterparts. From the first Matt  -decomposition of the Weyl tensor, it is easy to get [33]

$$R_{\alpha\beta\gamma\delta} = C_{\alpha\beta\gamma\delta} + \frac{1}{2}(g_{\alpha\gamma}R_{\beta\delta} - g_{\beta\gamma}R_{\alpha\delta} - g_{\alpha\delta}R_{\beta\gamma} + g_{\beta\delta}R_{\alpha\gamma}) - \frac{1}{6}(g_{\alpha\gamma}g_{\beta\delta} - g_{\alpha\delta}g_{\beta\gamma})R. \quad (7)$$

Therefore,  $K_1$ ,  $K_2$  and  $K_3$  can be expressed as follows

$$\begin{aligned} K_1 &= C_{\alpha\beta\gamma\delta}C^{\alpha\beta\gamma\delta} + 2R_{\alpha\beta}R^{\alpha\beta} - \frac{1}{3}R^2 = \\ &= I_1 + 2R_{\alpha\beta}R^{\alpha\beta} - \frac{1}{3}R^2, \\ K_2 &= [*C]_{\alpha\beta\gamma\delta}C^{\alpha\beta\gamma\delta} = I_2 \\ K_3 &= -C_{\alpha\beta\gamma\delta}C^{\alpha\beta\gamma\delta} + 2R_{\alpha\beta}R^{\alpha\beta} - \frac{2}{3}R^2 = \\ &= -I_1 + 2R_{\alpha\beta}R^{\alpha\beta} - \frac{2}{3}R^2. \end{aligned} \quad (8)$$

From the above equations it is straightforward to infer the explicit expressions of the second order invariants in a FRW universe:

$$\begin{aligned} I_1 &= \frac{60}{c^4} \left\{ (\dot{H} + 2H^2)^2 + H^4 + \frac{2H^2kc^2}{R_0^2a^2} + \frac{k^2c^4}{R_0^4a^4} \right\}, \\ I_2 &= 0, \\ I_3 &= -\frac{12}{c^4} \left\{ 5(\dot{H} + 2H^2)^2 + 5H^4 + \frac{10kc^2H^2}{R_0^2a^2} + \frac{5k^2c^4}{R_0^4a^4} \right. \\ &\quad \left. + 2(\dot{H} + 2H^2)H^2 + 2(\dot{H} + 2H^2)\frac{kc^2}{R_0^2a^2} \right\}. \end{aligned} \quad (9)$$

The HP postulate reads

$$\rho_X = \frac{3\alpha}{8\pi G} \sqrt{|I_i|}, \quad i = 1, 2, 3; \quad (10)$$

where  $\alpha$  is an dimensionless constant and should not be confused with the tensorial index.

By combining together eqs. (10) and (1) and by using the above expressions for  $I_1$  and  $I_3$  (the only two non-trivial invariants), we obtain two differential equations, each one providing the temporal evolution of the Hubble parameter. A first interesting step consists in solving the associated differential equations numerically for both  $I_1$  and  $I_3$ , finding the correspondent acceleration parameters, by using the definition

$$q(t) = -\frac{\ddot{H}}{H^2} - 1, \quad (11)$$

and the effective barotropic parameters, expressed by

$$w(t) = -1 - \frac{1}{3H} \frac{d}{dt} \ln \rho, \quad (12)$$

for both the models.

From now on, we will refer to the cosmological models arising from the invariants  $I_1$  and  $I_3$  as *mod*<sub>1</sub> and *mod*<sub>3</sub>,

respectively. In order to fix the free parameters of our two models, we need to find for which values of  $\alpha$ , the conditions  $q_0 < 0$  and  $w \sim -1$  at redshift  $z = 0$  are fulfilled. The corresponding intervals are  $\alpha \in [0.042, 0.052]$  and  $\alpha \in [0.039, 0.047]$  for *mod*<sub>1</sub> and *mod*<sub>3</sub> respectively. In figures 1, 2, 3 and 4 we plot  $q(z)$  and  $w(z)$  as functions of the redshift for both *mod*<sub>1</sub> and *mod*<sub>3</sub>. As shown in the pictures, if we set  $\alpha = 0.050$  for *mod*<sub>1</sub> and  $\alpha = 0.046$  for *mod*<sub>3</sub> we get the expected accelerated behavior of the universe, being  $q \sim -0.6$  and  $w \sim -1$ . In particular, the results obtained with the two models suggest that the universe is accelerating since  $z \sim 0.4$ .

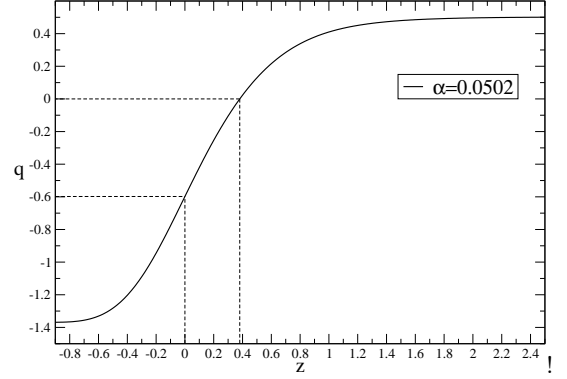


FIG. 1. Deceleration parameter  $q$  as a function of the redshift  $z$  for *mod*<sub>1</sub> (in this case we use conventionally  $\alpha = 0.050$ ). Note that  $q$  is negative for  $z < 0.4$ , providing an accelerated behavior of the universe since  $z = 0.4$ ; this is quite in agreement with the prediction of  $\Lambda$ CDM which refers to  $z \sim 0.77$ .

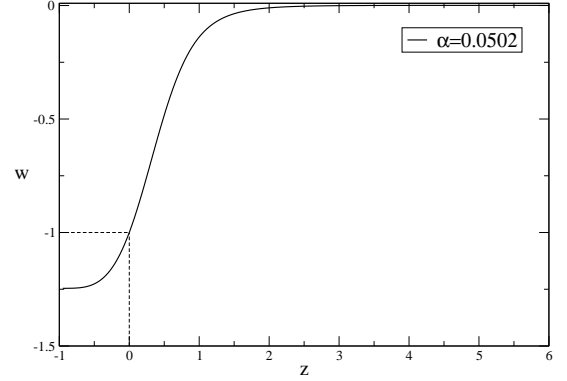


FIG. 2. The barotropic factor  $w \equiv \frac{p}{\rho}$  as a function of the redshift  $z$  for *mod*<sub>1</sub> (in this case we use  $\alpha = 0.050$ ). Notice that  $w = -1$  at  $z = 0$ , behaving as a cosmological constant at low redshift.

Once determined  $q(z)$  and  $w(z)$  we can characterize completely the kinematics of the models. In the following section we will check the agreement of our models with the observations. In particular, we will make use of three independent tests: SNeIa, BAO and CMB.

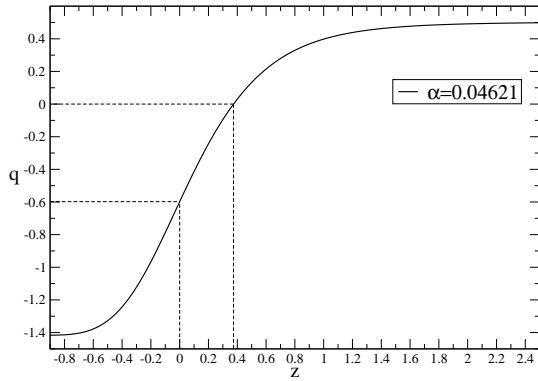


FIG. 3. Deceleration parameter  $q$  as a function of the redshift  $z$  for  $mod_3$  (in this case we use  $\alpha = 0.046$ ). Again  $q$  is negative for  $z < 0.4$ , providing an accelerated behavior of the universe since  $z = 0.4$  until now.

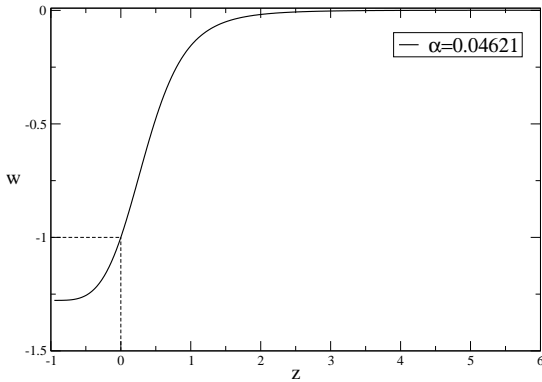


FIG. 4. The barotropic factor  $w$  as a function of the redshift  $z$  for  $mod_3$  (in this case we use  $\alpha = 0.046$ ). Notice that again  $w = -1$  at  $z = 0$ , behaving in this case too as a cosmological constant term at low redshift.

### III. COSMOLOGICAL CONSTRAINTS

In this section we perform an experimental combined procedure, by using a fairly typical combination of kinematical data. In particular we employ the three most common fitting procedures: SNeIa, BAO and CMB; the first two concern low redshift data sets spanning from  $z = 0$  to  $z \sim 2$ , while the third is a higher redshift test, since it is performed at  $z \sim 1000$ .

It is well established that standard candle data from SNeIa are indicators of distance, able to fit the correspondent luminosity distances for a particular class of models, by considering the distance modulus and the correspondent redshift  $z$ . The problem of the systematics, which usually affects these measures, can be avoided or at least reduced, by the use of the most recent updated Union 2 compilation [34], instead of other older samples [35]. Then, associating to each Supernova modulus  $\mu$  the corresponding  $1\sigma$  error, denoted by  $\sigma_\mu$ , we can perform directly the experimental analysis. To this purpose, let

us rewrite the distance modulus

$$\mu = 25 + 5 \log_{10} \frac{d_L}{\text{Mpc}}, \quad (13)$$

where  $d_L(z)$  is the luminosity distance, defined by

$$d_L(z) = c(1+z) \int_0^z \frac{dz'}{H(z')}. \quad (14)$$

Since the likelihood function  $\mathcal{L}$  is related to the chi-square statistic, i.e.  $\mathcal{L} \propto \exp(-\chi^2/2)$ , we constrain the free parameters of a model, by minimizing the quantity

$$\chi_{SN}^2 = \sum_i \frac{(\mu_i^{\text{theor}} - \mu_i^{\text{obs}})^2}{\sigma_i^2}. \quad (15)$$

The second test that we perform is related to the observations of large scale galaxy clusterings, which provide the signatures of the BAO [36]. In particular we use the measurement of the peak of luminous red galaxies observed in Sloan Digital Sky Survey (SDSS), usually denoted by  $A$  and defined as follows

$$A = \sqrt{\Omega_m} \left[ \frac{H_0}{H(z_{BAO})} \right]^{\frac{1}{3}} \left[ \frac{1}{z_{BAO}} \int_0^{z_{BAO}} \frac{H_0}{H(z)} dz \right]^{\frac{2}{3}}, \quad (16)$$

with  $z_{BAO} = 0.35$ . In addition, the observed  $A$  is estimated to be

$$A_{obs} = 0.469 \left( \frac{0.95}{0.98} \right)^{-0.35}, \quad (17)$$

with an error  $\sigma_A = 0.017$ . In the case of the BAO measurement we should perform the following minimization:

$$\chi_{BAO}^2 = \left( \frac{A - A_{obs}}{\sigma_A} \right)^2. \quad (18)$$

Finally, concerning the CMB, we first analyze the so-called CMB shift parameter

$$R = \sqrt{\Omega_m} \int_0^{z_{CMB}} \frac{H_0}{H(z)} dz. \quad (19)$$

Since this standard ruler is fixed by the sound horizon at decoupling ( $z_{\text{dec}} = 1091.36$  [37]), it gives a complementary bound to the SNeIa data and BAO as well. For the  $R$  parameter, the observed value is  $R_{obs} = 1.726 \pm 0.018$ , as inferred from the WMAP 7 data [34]. Hence, the correspondent CMB constraints are given by minimizing the chi square

$$\chi_{CMB}^2 = \left( \frac{R - R_{obs}}{\sigma_R} \right)^2. \quad (20)$$

Moreover, we notice that, differently from SNeIa, BAO and CMB do not depend on  $H_0$ .

Finally, by combining the minimization procedures for SNeIa, CMB and BAO, we constrain the parameters of

$\Omega_m(SN)$	$\Omega_m(BAO)$	$\Omega_m(CMB)$
$0.240 \pm 0.070$	$0.234 \pm 0.014$	$0.266 \pm 0.064$
$\alpha(SN)$	$\alpha(BAO)$	$\alpha(CMB)$
$0.046 \pm 0.016$	$0.044 \pm 0.010$	$0.025 \pm 0.016$

TABLE I. Summary of the results for  $mod_1$ ; in this case we have  $\chi^2_{SNeIa} = 1.021$ ,  $\chi^2_{BAO} = 1.001$ ,  $\chi^2_{CMB} = 1.001$ ,  $\Omega_{m,(mean)} = 0.247 \pm 0.070$ ,  $\alpha_{(mean)} = 0.038 \pm 0.016$ .

$\Omega_m(SN)$	$\Omega_m(BAO)$	$\Omega_m(CMB)$
$0.260 \pm 0.090$	$0.312 \pm 0.080$	$0.343 \pm 0.060$
$\alpha(SN)$	$\alpha(BAO)$	$\alpha(CMB)$
$0.042 \pm 0.010$	$0.042 \pm 0.002$	$0.024 \pm 0.0015$

TABLE II. Summary of the results for  $mod_3$ . The reduced chi squared are  $\chi^2_{SNeIa} = 1.021$ ,  $\chi^2_{BAO} = 1.001$ ,  $\chi^2_{CMB} = 1.003$ ; the mean values  $\Omega_{m,(mean)} = 0.305 \pm 0.090$ ,  $\alpha_{(mean)} = 0.036 \pm 0.015$ .

our two models. The numerical results are summarized in the following tables:

The results show that the theoretical predictions discussed in Sec.II are in agreement with the experimental ones. The mean values of  $\alpha$  in the tables are indeed included in the intervals of values found in Sec.II. The CMB measurements are usually smaller if compared with the SNeIa and BAO ones. Notice finally that for the SNeIa we had to fix a value for  $H_0$  ( $H_0 = 2.33^{-18} s^{-1}$ ), while for CMB and BAO it is not necessary.

#### IV. COMPARISON WITH OTHER MODELS

In the Introduction we pointed out that the  $\Lambda$ CDM paradigm appears to be the favorite fitting model among a large number of possibilities. This should depend on its small number of parameters. In particular, for a flat cosmology, the only parameter involved is the mass density  $\Omega_m$ .

Therefore, one can ask if there is a real necessity to go beyond this approach, by considering other frameworks. This question suggests the requirement to find a test able to compare different cosmological models, in order to select the "best" one. At the same time, such a test should also be model independent.

A good choice is represented by the so-called Akaike Information Criterion (AIC) and BIC [38, 39] tests, which are two of the most model-independent statistical methods for comparing different models. Moreover, since their first use by Liddle [40], these tests became a standard diagnostic tool [41–43] of regression models [44–47].

The idea behind AIC is based on postulating two distribution functions, namely  $f(x)$  and  $g(x|\theta)$ :  $f(x)$  is assumed to be the exact one, while  $g(x|\theta)$  approximates the former through a set of parameters denoted by  $\theta$ . Hence,

once given  $f(x)$  and  $g(x|\theta)$ , there exists only a set of  $\theta_{min}$  minimizing the difference between  $g(x, \theta)$  and  $f(x)$  [48].

However, without going into details, we only note that the AIC value for a single model is meaningless since the exact model function  $f(x)$  is unknown. Therefore, the quantities of interest are the differences  $\Delta AIC \equiv AIC - AIC_{min}$ , calculated over the whole set of models. The generic AIC is given by

$$AIC = -2 \ln \mathcal{L}_{max} + 2\kappa. \quad (21)$$

A very similar criterion was derived by Schwarz [45] in a Bayesian context (see [46] and references therein).

The BIC test provides

$$BIC = -2 \ln \mathcal{L}_{max} + k \ln N, \quad (22)$$

where, for both AIC and BIC,  $\mathcal{L}_{max}$  is the maximum likelihood,  $k$  is the number of parameters, and  $N$  is the number of data points used in the fit. If the errors are Gaussian, then  $\chi^2_{min} = -2 \ln \mathcal{L}_{max}$  and the difference in BIC can be simplified to  $\Delta BIC = \Delta \chi^2_{min} + \Delta k \ln N$ .

We adopted both the AIC and BIC tests for different models.

A first natural extension of the  $\Lambda$ CDM paradigm is the  $w$ CDM model, also called quintessence model; it provides an EoS of the form  $p = w\rho$  with a negative barotropic factor, whose origin is related to the coupling of the Ricci scalar with a not evolving scalar field  $\phi$ . Since this model is strongly dependent on  $w$ , it is called  $w$ CDM in analogy with the  $\Lambda$ CDM.

The theoretical explanation about the origin of the scalar field giving a negative EoS remains unsolved in the  $w$ CDM, then a varying quintessence has been proposed: if  $w$  evolves with the redshift  $z$ , i.e.  $w = w[z]$ , the scalar field evolves as well. So the origin of the latter should be found thermodynamically or in other ways.

One of the more recent and intriguing varying quintessence model has been proposed by the Chevallier, Polarsky, Linder (CPL) [49]. This parametrization suggests that  $w[a] = w_0 + w_1(1-a)$ . Assuming  $a \equiv (1+z)^{-1}$ , one gets  $w[z] = w_0 + w_1 \frac{z}{1+z}$ , which for low and very high redshifts becomes constant, i.e.  $w(z \rightarrow 0) = w_0$  and  $w[z \rightarrow \infty] = w_0 + w_1$ .

We perform the AIC and BIC tests for our two models ( $mod_1$  and  $mod_3$ ) and for the models discussed above. Moreover, we also include the Ricci DE model (RDE), studied by Gao [23]. The normalized Hubble rates,  $E \equiv \frac{H}{H_0}$ , for these models are written below (notice that there is not an analytic expression of  $E$  for the models  $mod_1$

and  $mod_3$ ):

$$\begin{aligned}
E_{\Lambda CDM} &= \sqrt{\Omega_m(z) + 1 - \Omega_m}, \\
E_{wCDM} &= \sqrt{\Omega_m(z) + (1 - \Omega_m)(1 + z)^{3(1+w)}}, \\
E_{CPL} &= \sqrt{\Omega_m(z) + (1 - \Omega_m)f(z)}, \\
E_{RDE} &= \sqrt{\frac{2}{2 - \alpha}\Omega_m(z) + \Omega_f(1 + z)^{4 - \frac{2}{\alpha}}},
\end{aligned} \tag{23}$$

where  $f(z) = (1 + z)^{3(1+w_0+w_1)} \exp\left\{-\frac{3w_1z}{1+z}\right\}$  and  $\Omega_m(z) \equiv \Omega_m(1 + z)^3$ .

The results of the tests are summarized in the table below, in which we report, for each model, the number and the names of the free parameters, the  $\chi^2$  and the values of BIC and AIC:

Model	N. Par. (k-1)	Param.	$\chi^2_{min}$	$\Delta BIC$	$\Delta AIC$
$\Lambda CDM$	1	$\Omega_m$	557.40	0	0
Quint.	2	$\Omega_m, w$	557.28	6.20	1.88
CPL	3	$\Omega_m, w_0, w_a$	557.45	12.69	4.05
RDE	2	$\Omega_m, \alpha$	573.72	22.64	18.32
$mod_1$	2	$\Omega_m, \alpha$	568.86	17.79	13.46
$mod_3$	2	$\Omega_m, \alpha$	568.91	17.84	13.51

where we have used:  $\Omega_m = 0.254 \pm 0.038$  for  $\Lambda CDM$ ;  $\Omega_m = 0.325 \pm 0.049$  and  $w = -1.18 \pm 0.18$  for  $wCDM$ ;  $\Omega_m = 0.246 \pm 0.034$ ,  $w_0 = -0.91 \pm 0.12$  and  $w_a = -0.32 \pm 0.04$  for CPL [50, 51];  $\Omega = 0.310 \pm 0.052$  and  $\alpha = 0.380 \pm 0.049$  for the Ricci DE.

The results have been obtained through a direct analysis of each model, following the combined procedure explained in Section III. We can conclude that our models are disfavored by the AIC and BIC analysis if compared with  $\Lambda CDM$  and  $wCDM$ . It is clear that  $\Lambda CDM$  remains the favorite model. On the other hand, the results obtained for the Ricci DE are even worst. This seems to suggest that using higher order invariants is better than using invariants of lower order, encouraging further investigations in our direction. Concerning the CPL model,

it is interesting to notice that, to a slight variation of  $w_0$  and  $w_a$ , it corresponds a large variation of AIC and BIC. This is in agreement with the fact that CPL is a three parameters approach, then it appears disfavored if compared with  $mod_1$  and  $mod_3$ .

## V. CONCLUSION

In this work we have investigated the possibility to relate the DE term with the second order independent invariants  $I_i$ . This has been performed in analogy with the work of Gao [23], who proposed a first order invariant approach, namely the Ricci DE. The validity of our idea is based on the holographic principle, which requires the existence of a cut-off scale, characterizing the dark energy. Moreover, the latter must scale with the inverse square of the cut-off (which means  $\rho_X \propto \sqrt{I_i}$ ). After solving numerically the Friedmann equations for the two non-trivial invariants in a flat FRW universe, we tested the two resulting models, namely  $mod_1$  and  $mod_3$ . Hence, we first analyzed the kinematics of the two models in terms of the acceleration parameter  $q(z)$  and in terms of the barotropic factor  $w(z)$ , showing that they are compatible with the conditions  $q < 0$  and  $w \sim -1$  at  $z = 0$ . Then, we developed a test combining SNeIa, BAO and CMB in order to fix the cosmological parameters; again in this case we found a good agreement with the experimental results. It is also important to notice that the two models, arising from different invariants, show an incredibly similar behavior.

A robust evidence of the validity of the models is given by the AIC and BIC tests, where we get results better than those obtained with the Ricci DE approach. Therefore, our models are compatible with the holographic principle and seem to behave better than the first order invariant proposed by Gao. This encourages to study higher order invariants, what will be done in future works.

## ACKNOWLEDGEMENTS

It is a pleasure to thank Prof. Luca Amendola, Dr. Andrea Geralico, Prof. Salvatore Capozziello and Prof. Hernando Quevedo for very fruitful discussions.

---

[1] A. G. Riess et al., AJ, 116, 1009, (1998); S. Perlmutter et al., ApJ, 517, 565, (1999).  
[2] R. Rebolo et al., MNRAS, 353, 747, (2004); A. C. Pope et al., ApJ, 607, 655, (2004); P. McDonald et al., astro-ph/0405013, (2004).  
[3] M. Tegmark et al. (SDSS), Phys. Rev. D74, 123507 (2006); W. J. Percival et al., Mon. Not. Roy. Astron. Soc. 381,1053, (2007).

[4] L. Perivolaropoulos, arXiv:astro-ph/0601014; S. Nojiri and S. D. Odintsov, Int. J. Geom. Meth. Math. Phys. 4, 115, (2007); T. Padmanabhan, AIP Conf. Proc., 861, 179 (2006).  
[5] N. Straumann, Mod. Phys. Lett. A 21, 1083 (2006); S. Bludman, arXiv:astro-ph/0605198; J. P. Uzan, arXiv:astro-ph/0605313; D. Polarski, AIP Conf. Proc. 861, 1013 (2006); P. Ruiz-Lapuente, Class. Quant. Grav. 24, R 91,(2007).

